PHYSICAL REVIEW A **82**, 023416 (2010)

Atomic Siegert states in an electric field: Transverse momentum distribution of the ionized electrons

Pavel A. Batishchev,[1] Oleg I. Tolstikhin,[2] and Toru Morishita[3,4]
[1]*Moscow Institute of Physics and Technology, Institutskaya Street 9, Dolgoprudnyi 141700, Russia*
[2]*Russian Research Center "Kurchatov Institute," Kurchatov Square 1, Moscow 123182, Russia*
[3]*Department of Applied Physics and Chemistry, University of Electro-Communications, 1-5-1, Chofu-ga-oka, Chofu-shi, Tokyo, Japan*
[4]*PRESTO, Japan Science and Technology Agency, Kawaguchi, Saitama 332-0012, Japan*
(Received 11 May 2010; published 17 August 2010)

The Siegert states of atoms in a static uniform electric field, defined as the solutions to the stationary Schrödinger equation satisfying the regularity and outgoing-wave boundary conditions, are discussed. An efficient method to calculate not only the complex energy eigenvalue, but also the eigenfunction for a general class of one-electron atomic potentials is introduced. An exact expression for the transverse momentum distribution of the ionized electrons in terms of the Siegert eigenfunction in the asymptotic region is derived. The method is illustrated by calculations of the energy, ionization width, and transverse momentum distribution as functions of the electric field for several lowest states of H, outer p shells of Ne, Ar, Kr, and Xe, and the active electron in H^-. We also discuss the ionization of Ar by the pulse of a unidirectional time-dependent electric field, which illustrates the role of the Siegert states in the recently developed adiabatic theory of ionization of atoms by intense laser pulses [O. I. Tolstikhin *et al.*, Phys. Rev. A **81**, 033415 (2010)].

DOI: 10.1103/PhysRevA.82.023416 PACS number(s): 32.80.Fb, 32.80.Rm, 32.70.Jz

I. INTRODUCTION

When an atom is placed in a static uniform electric field **F**, the atomic electron (we restrict our consideration to the single-active-electron approximation) can be ionized. In weak fields, the electron escapes from the atom by tunneling through a potential barrier. The ionization rate in this case is exponentially small in F, so the atom survives in the initial bound state with an energy E_0 during many atomic periods $2\pi/|E_0|$ before ionization occurs. Thus one arrives at the concept of a quasistationary state. An important step in understanding the nature of quasistationary states in quantum mechanics, which enables one to exclude the influence of the initial conditions from the consideration and focus on the properties of the system *per se*, consists in associating them with the solutions to the stationary Schrödinger equation that have only outgoing waves in the asymptotic region [1]. The stationary Schrödinger equation supplemented by the regularity and outgoing-wave boundary conditions constitute an eigenvalue problem: The solutions exist only for a discrete set of generally complex values of the energy E of the system. This eigenvalue problem was first formulated by Siegert [2], so its solutions are called the Siegert states (SS's). A concise review of early studies on the theory of SS's can be found in [3]. The theory has been essentially advanced in [3–6], which has turned SS's into a powerful tool in stationary scattering calculations [7–16]. Applications of SS's to nonstationary problems are discussed in [17–20]. Quasistationary states are represented by the SS's for which $\mathrm{Im}E < 0$ and $|\mathrm{Im}E| \ll |\mathrm{Re}E|$. The SS's of an atom in an electric field, also known as the Stark or LoSurdo-Stark states, are the subject of the present paper. The SS that for $F = 0$ coincides with the initial bound state in the tunneling regime represents the quasistationary state mentioned above. In sufficiently strong fields the electron can fly away through a classically accessible window over the potential barrier. In this case, ionization occurs during one atomic period, so the initial bound state does not describe the system even approximately. Meanwhile, the corresponding SS can be analytically continued to any value of F. Whether this state preserves some physical meaning in the overbarrier regime, when $|\mathrm{Im}E| \sim |\mathrm{Re}E|$, is one of the questions to be discussed in the following.

One of the major characteristics of an atomic SS in an electric field is its complex energy eigenvalue E as a function of F. In the tunneling regime, the calculation of the real part of the difference $E - E_0$ defining the Stark shift is a textbook application of perturbation theory [21]. Of main interest is finding the imaginary part of E that defines the ionization rate. The theoretical study of the field ionization of atoms was pioneered by Oppenheimer [22]. Lanczos was the first who applied the asymptotic approach to the solution of the problem in the limit $F \to 0$ [23]. The correct asymptotic result for the ionization rate from the hydrogen atom in the ground state, including the pre-exponential factor, was obtained in [21]. The approach of [21] was later extended to the hydrogen atom in an arbitrary bound state [24]. The extension was not straightforward; Ref. [24] contains an interesting review of errors made in earlier asymptotic treatments of the problem. There exists an extensive literature devoted to exact calculations of the Siegert eigenvalues E for the different states of the hydrogen atom beyond the tunneling regime by various analytical and numerical methods [25–34]. The hydrogen atom occupies a special position in studies of the SS's, because the Schrödinger equation in this case allows separation of variables in parabolic coordinates [21]. This greatly facilitates the calculations and even makes the analysis of the global structure of the Riemann surface of E as a multivalued analytic function of F possible [35]. Another problem that allows an accurate asymptotic [36] and numerical [37] treatment is the field ionization from a zero-range potential, which is often used to model negative atomic ions [38]. Some calculations by the complex rotation method [28,39] of the ionization rates for potentials with a non-Coulombic core modeling many-electron atoms and ions are also available [40].

A uniform electric field infinitely accelerates the ionized electrons in the direction parallel to the field, but their transverse momentum distribution (TMD) gets stabilized as they recede from the atom. The TMD of the ionized electrons is another important characteristic of the SS. However, we are not aware of any calculations of TMD's in the stationary framework. To fill in this gap is one of the goals of this paper.

The SS's also emerge in the nonstationary context in studies of the laser-atom interaction. Indeed, one can expect that ionization of atoms by an alternating electric field of sufficiently low frequency proceeds in the same way as in a static field. One of the most widely used theory of ionization of atoms by intense laser fields was proposed by Keldysh [41]. In the development of this theory, analytical expressions for the momentum distribution of photoelectrons were obtained [42,43], for details see a review article [44]. In the low-frequency limit, which corresponds to small values of the Keldysh parameter γ, the results of [42,43] yield a formula for the ionization rate from an arbitrary n^*lm state, where n^* is an effective principal quantum number accounting for a non-Coulombic core of the atomic potential [44]. For the hydrogen atom in the ground state, this formula coincides (apart from averaging over the laser period) with the $F \to 0$ limit of the ionization rate in a static field [21]. It extends the asymptotic results of [21,24,36] to a more general class of potentials. Another result following from [42,43] in the limit $\gamma \to 0$ is a universal for $m = 0$ (i.e., independent of l and details of the atomic potential) Gaussian shape of the TMD with the width $(F/\varkappa)^{1/2}$, where $\varkappa = (2|E_0|)^{1/2}$. These results were later reproduced by other authors [45,46] and became known as the Ammosov-Delone-Krainov theory; a history of the problem is discussed in [47]. Thus a nonstationary Keldysh theory has shed, implicitly, some new light on the properties of stationary SS's. It should be emphasized that the Keldysh theory, and hence the results of [42,43,45,46], are valid only for sufficiently weak fields $F \ll \varkappa^3$ [44], which in the low-frequency limit corresponds to the tunneling regime of ionization.

The field ionization is the first step for a variety of processes taking place in the interaction of atoms with intense infrared laser pulses [48,49]. An accurate description of the photoelectron wave packets created during each unidirectional half-cycle of the laser field is necessary for the analysis and prediction of experimentally observable photoelectron and harmonic generation spectra as well as for retrieving from such spectra the structural target information [50–52]. Lasers operating both in the tunneling and overbarrier regimes of ionization are currently available; a crossover between the two regimes for neutral atoms in the ground state occurs at intensities $I \sim 10^{15}$ W/cm^2. Thus a theory capable of quantitatively treating the intermediate and overbarrier regimes, where the Keldysh-type theories [48,49] are valid only qualitatively or do not apply at all, is needed.

Recently, we have initiated the development of the adiabatic theory of ionization of atoms by intense laser pulses [53]. This theory rests on a single parameter ϵ giving a ratio of the atomic and laser time scales and becomes exact in the limit $\epsilon \to 0$ *uniformly* with respect to the amplitude of the laser pulse, that is, it applies to weak as well as strong fields provided that ϵ is sufficiently small. For neutral atoms in the ground state ($|E_0| \sim 13.6$ eV) and infrared laser pulses of current interest ($\lambda \sim 800$ nm, $\omega \sim 1.5$ eV) we have $\epsilon \sim \omega/|E_0| \sim 0.1$, so the adiabatic theory should work well. A central object in this theory is the SS that for $F = 0$ coincides with the initial bound state of the target atom. The solution to the time-dependent Schrödinger equation and resulting photoelectron spectrum is expressed in terms of this state analytically continued to certain generally complex values of F. In the one-dimensional zero-range potential model considered in [53], the SS in question can be easily calculated by solving a transcendental equation, see Appendix C therein. To implement the adiabatic theory [53] for realistic atomic potentials in three dimensions, one needs to construct the corresponding SS. To address this issue and thus to prepare grounds for further development [54] of the adiabatic theory is the main goal of this work.

In the present paper, we introduce an efficient approach to constructing the SS's for a general class of atomic potentials. The approach is based on the slow-variable discretization method [55] in combination with the R-matrix propagation technique [56]. It enables one to obtain not only the complex energy eigenvalue E, but also the properly normalized eigenfunction and hence the TMD of the ionized electrons. The approach is illustrated by calculations of the energy, ionization width, and TMD as functions of the electric field F for a number of typical atomic potentials. As a preliminary illustration of future applications of the SS's in the adiabatic theory [53,54], we also discuss one nonstationary problem, namely, the ionization of Ar by a half-cycle laser pulse of overbarrier intensity.

II. BASIC EQUATIONS

The stationary Schrödinger equation describing an electron interacting with an atomic potential $V(\mathbf{r})$ and a static uniform electric field $\mathbf{F} = F\mathbf{e}_z$ reads (atomic units are used throughout the paper)

$$\left[-\tfrac{1}{2}\Delta + V(\mathbf{r}) + Fz - E\right]\psi(\mathbf{r}) = 0. \tag{1}$$

The SS's are represented by the regular solutions to this equation which have only outgoing waves in the asymptotic region; a precise formulation of these boundary conditions is given in the next section. Let for $F = 0$ Eq. (1) have solutions corresponding to bound states of the unperturbed atom. For $F > 0$, these solutions turn into the SS's we are interested in. In contrast to Refs. [3–6], where we have dealt with a complete set of SS's, here we consider only one particular SS that originates from a given bound state with the energy E_0. In the following, E and $\psi(\mathbf{r})$ denote the corresponding eigenvalue and eigenfunction; one should remember that these as well as other characteristics of the SS introduced in the following depend on F, which for brevity is not indicated explicitly. The atomic potential $V(\mathbf{r})$ may have a finite-range core, maybe with the Coulomb singularity at $r \to 0$, and an asymptotic Coulomb tail at $r \to \infty$. We restrict our consideration to axially symmetric potentials. It is convenient to use parabolic coordinates defined by

$$\xi = r + z, \quad 0 \leqslant \xi < \infty, \tag{2a}$$

$$\eta = r - z, \quad 0 \leqslant \eta < \infty. \tag{2b}$$

Then our assumptions concerning $V(\mathbf{r})$ can be formalized as follows:

$$V(\mathbf{r}) = V(\xi,\eta), \tag{3a}$$

$$V(\xi,\eta)|_{\eta>\eta_c} = -\frac{Z_{\rm as}}{r}, \quad r = \frac{\xi+\eta}{2}. \tag{3b}$$

The parameter η_c defining the boundary of the core is introduced to simplify the formulation; it is understood that convergence of the results with respect to this parameter is to be achieved in the calculations. The asymptotic charge $Z_{\rm as}$ characterizes the Coulomb tail. Local spherically symmetric one-electron potentials in use to model neutral atoms and atomic ions [57,58] comply with Eq. (3). The hydrogen atom presents a special case in which the core is absent and Eq. (3b) with $Z_{\rm as} = 1$ applies throughout the interval (2b).

The solution to Eq. (1) will be sought in the form

$$\psi(\mathbf{r}) = \frac{e^{im\varphi}}{\sqrt{2\pi}}\psi(\xi,\eta), \tag{4}$$

where φ, $0 \leqslant \varphi < 2\pi$, is the azimuthal angle of $\mathbf{r}$ about the z axis, and $m = 0, \pm 1, \pm 2, \ldots$, is the magnetic quantum number of the unperturbed bound state. The Schrödinger equation for $\psi(\xi,\eta)$ reads [21]

$$\left[\frac{\partial}{\partial\eta}\eta\frac{\partial}{\partial\eta} - \frac{m^2}{4\eta} + \mathcal{B}(\eta) + \frac{E\eta}{2} + \frac{F\eta^2}{4}\right]\psi(\xi,\eta) = 0, \tag{5}$$

where

$$\mathcal{B}(\eta) = \frac{\partial}{\partial\xi}\xi\frac{\partial}{\partial\xi} - \frac{m^2}{4\xi} - \frac{\xi+\eta}{2}V(\xi,\eta) + \frac{E\xi}{2} - \frac{F\xi^2}{4}, \tag{6}$$

is an operator acting on functions of ξ and depending on η as a parameter. The real and imaginary parts of the eigenvalue E define the energy and ionization width of the SS,

$$E = \mathcal{E} - \frac{i}{2}\Gamma. \tag{7}$$

The eigenfunction will be normalized by

$$\frac{1}{4}\int_0^\infty\int_0^\infty \psi^2(\xi,\eta)(\xi+\eta)\,d\xi d\eta = 1. \tag{8}$$

This formally coincides with the normalization condition for bound states [21]. However, for $F > 0$, $\psi(\xi,\eta)$ exponentially grows in the asymptotic region, so the integral in Eq. (8) does not converge in the usual sense of the word and requires a regularization. Note that there is no complex conjugation in Eq. (8), which is a general property of the theory of SS's [2–6].

III. ADIABATIC EXPANSION IN PARABOLIC COORDINATES

Let us introduce the adiabatic basis defined by

$$\mathcal{B}(\eta)\phi_\nu(\xi;\eta) = \beta_\nu(\eta)\phi_\nu(\xi;\eta), \quad \nu = 0,1,2\ldots, \tag{9a}$$

$$\phi_\nu(\xi;\eta)|_{\xi\to 0} \propto \xi^{|m|/2}, \quad \phi_\nu(\xi;\eta)|_{\xi\to\infty} = 0. \tag{9b}$$

Since the operator $\mathcal{B}(\eta)$ depends on E, the solutions to Eq. (9) are generally complex. We order them by the number of zeros ν (excluding the one at $\xi = 0$ for $|m| > 0$) in the limit $F \to 0$, when E converges to E_0 and becomes real. The eigenvalues $\beta_\nu(\eta)$ and eigenfunctions $\phi_\nu(\xi;\eta)$ of $\mathcal{B}(\eta)$ depend on η as a parameter (the term "adiabatic" is traditionally used to indicate this dependence, it has nothing to do with adiabaticity in time). For any η in the interval (2b), the different eigenfunctions are orthogonal and we normalize them by

$$\langle\phi_\nu(\xi;\eta)|\phi_\mu(\xi;\eta)\rangle \equiv \int_0^\infty \phi_\nu(\xi;\eta)\phi_\mu(\xi;\eta)\,d\xi = \delta_{\nu\mu}. \tag{10}$$

Similarly to adiabatic expansions in the Born-Oppenheimer treatment of diatomic molecules [59] and hyperspherical treatments of three-body Coulomb systems [60,61] and chemical reactions [62,63], the solution to Eq. (5) can be sought in the form

$$\psi(\xi,\eta) = \sum_\nu f_\nu(\eta)\phi_\nu(\xi;\eta). \tag{11}$$

Substituting this expansion into Eq. (5), one obtains a set of coupled ordinary differential equations defining the coefficient functions $f_\nu(\eta)$,

$$\left[\frac{d}{d\eta}\eta\frac{d}{d\eta} - \frac{m^2}{4\eta} + \beta_\nu(\eta) + \frac{E\eta}{2} + \frac{F\eta^2}{4}\right]f_\nu(\eta) + \sum_\mu\left[P_{\nu\mu}(\eta)\left(2\eta\frac{d}{d\eta}+1\right) + \eta Q_{\nu\mu}(\eta)\right]f_\mu(\eta) = 0, \tag{12}$$

where

$$P_{\nu\mu}(\eta) = \left\langle\phi_\nu(\xi;\eta)\middle|\frac{\partial\phi_\mu(\xi;\eta)}{\partial\eta}\right\rangle, \tag{13a}$$

$$Q_{\nu\mu}(\eta) = \left\langle\phi_\nu(\xi;\eta)\middle|\frac{\partial^2\phi_\mu(\xi;\eta)}{\partial\eta^2}\right\rangle. \tag{13b}$$

The regular solutions to Eq. (12) satisfy

$$f_\nu(\eta)|_{\eta\to 0} \propto \eta^{|m|/2}. \tag{14}$$

According to Eq. (3b), the adiabatic basis ceases to depend on η for $\eta > \eta_c$. We also introduce the asymptotic basis defined by

$$\beta_\nu = \beta_\nu(\eta)|_{\eta>\eta_c}, \quad \phi_\nu(\xi) = \phi_\nu(\xi;\eta)|_{\eta>\eta_c}, \tag{15}$$

or explicitly,

$$\left[\frac{d}{d\xi}\xi\frac{d}{d\xi} - \frac{m^2}{4\xi} + Z_{\rm as} + \frac{E\xi}{2} - \frac{F\xi^2}{4}\right]\phi_\nu(\xi) = \beta_\nu\phi_\nu(\xi), \tag{16a}$$

$$\phi_\nu(\xi)|_{\xi\to 0} \propto \xi^{|m|/2}, \quad \phi_\nu(\xi)|_{\xi\to\infty} = 0. \tag{16b}$$

Note, importantly, that the solutions $\phi_\nu(\xi)$ do not depend on $Z_{\rm as}$, and hence are universal functions of ξ for all potentials of the type (3). Also note that these functions depend on E and F only via a combination $FE^{-3/2}$, which can be seen by rescaling the independent variable. For $\eta > \eta_c$, the coupling matrices (13) vanish and Eq. (12) takes the form

$$\left[\frac{d^2}{d\eta^2} + \frac{1-m^2}{4\eta^2} + \frac{\beta_\nu}{\eta} + \frac{E}{2} + \frac{F\eta}{4}\right]\eta^{1/2}f_\nu(\eta) = 0. \tag{17}$$

For $F > 0$ and $\arg F = 0$, the outgoing-wave solutions to these uncoupled equations satisfy

$$f_\nu(\eta)|_{\eta\to\infty} = f_\nu f(\eta), \tag{18a}$$

$$f(\eta) = \frac{2^{1/2}}{F^{1/4}\eta^{3/4}} \exp\left[\frac{iF^{1/2}\eta^{3/2}}{3} + \frac{iE\eta^{1/2}}{F^{1/2}}\right]. \tag{18b}$$

This asymptotic does not depend on the channel eigenvalue β_ν, that is, apart from a constant coefficient f_ν, it is the same for all channels. Substituting Eq. (18a) into Eq. (11), we obtain

$$\psi(\xi,\eta)|_{\eta\to\infty} = f(\eta)\phi(\xi), \tag{19}$$

where

$$\phi(\xi) = \sum_\nu f_\nu \phi_\nu(\xi). \tag{20}$$

Thus, independently of the atomic potential, the outgoing-wave solution to Eq. (5) acquires a separable form in the asymptotic region. For the hydrogen atom, the adiabatic basis does not depend on η and is determined by Eq. (16) throughout the interval (2b), and only one term is present in expansions (11) and (20) with $f_\nu(\eta)$ defined by Eqs. (14), (17), and (18).

Equations (9b), (14), and (18) specify the regularity and outgoing-wave boundary conditions defining the SS's. Equations (14) and (18) can be satisfied simultaneously only for special values of E, so we deal with an eigenvalue problem. The eigenvalue E is complex and $\mathrm{Im}E < 0$, so the eigenfunction (19) exponentially grows with η. We now can regularize the integral in Eq. (8). This can be done by deforming the integration path in η from the real semiaxis $[0,\infty)$ into a contour $\mathcal{C}$ in the complex η plane that runs to infinity inside the sector $0 < \arg\eta < 2\pi/3$. For example, one can use

$$\mathcal{C} = [0,\eta_c] + [\eta_c, e^{i\pi/3}\times\infty). \tag{21}$$

The function $\psi(\xi,\eta)$ can be analytically continued from the real ray $\eta \in [\eta_c,\infty)$ to the complex part of this contour by analytically continuing Eq. (17); no analytic continuation of the atomic potential $V(\xi,\eta)$ is needed. We note in passing that this method of regularization of the normalization integral (8) agrees with a general procedure developed in [64].

IV. TRANSVERSE MOMENTUM DISTRIBUTION

There is a flux of probability associated with the SS $\psi(\mathbf{r})$ whose density $\mathbf{j}(\mathbf{r})$ satisfies

$$\nabla\mathbf{j}(\mathbf{r}) = \Gamma|\psi(\mathbf{r})|^2. \tag{22}$$

In the asymptotic region, this flux represents the ionized electrons which fly away from the atom in the direction opposite to that of the electric field. In this section we discuss the TMD in the outgoing flux.

A. General formula

For $F > 0$, the outgoing flux is directed toward $z \to -\infty$. The atomic potential $V(\mathbf{r})$ in Eq. (1) can be neglected for sufficiently large negative z. This holds also for potentials with the Coulomb tail, $Z_{\mathrm{as}} \neq 0$, since neither the function $f(\eta)$ nor asymptotic basis $\phi_\nu(\xi)$ depend on Z_{as}, and only the coefficients f_ν in Eqs. (19) and (20) depend on the potential. Then $\psi(\mathbf{r})$ in the asymptotic region can be presented in the form

$$\psi(\mathbf{r})|_{z\to-\infty} = \int A(\mathbf{k}_\perp)\, e^{i\mathbf{k}_\perp\mathbf{r}_\perp} g(z,k_\perp)\frac{d\mathbf{k}_\perp}{(2\pi)^2}, \tag{23}$$

where $\mathbf{r}_\perp = (x,y) = (r_\perp\cos\varphi, r_\perp\sin\varphi)$, $\mathbf{k}_\perp = (k_x,k_y) = (k_\perp\cos\chi, k_\perp\sin\chi)$, and

$$g(z,k_\perp) = e^{-i\pi/12} 2\pi^{1/2}(2F)^{-1/6}\mathrm{Ai}(\zeta), \tag{24a}$$

$$\zeta = \frac{2e^{-i\pi/3}}{(2F)^{2/3}}\left[E - Fz - \frac{k_\perp^2}{2}\right]. \tag{24b}$$

Here $\mathrm{Ai}(x)$ is the Airy function [65]. Thus the amplitude of ionization with the transverse momentum $\mathbf{k}_\perp$ is given by

$$A(\mathbf{k}_\perp) = \frac{1}{g(z,k_\perp)}\int \psi(\mathbf{r})\, e^{-i\mathbf{k}_\perp\mathbf{r}_\perp} d\mathbf{r}_\perp\bigg|_{z\to-\infty}. \tag{25}$$

Substituting Eq. (4) here, we obtain

$$A(\mathbf{k}_\perp) = \frac{e^{im\chi}}{\sqrt{2\pi}} A(k_\perp), \tag{26}$$

where

$$A(k_\perp) = \frac{2\pi e^{-im\pi/2}}{g(z,k_\perp)}\int_0^\infty \psi(\xi,\eta)J_m(k_\perp r_\perp)r_\perp dr_\perp\bigg|_{z\to-\infty}. \tag{27}$$

Equations (19) and (23) give two different representations of the same solution to Eq. (1) in the asymptotic region, so one can expect that the ionization amplitude $A(k_\perp)$ can be expressed in terms of the function $\phi(\xi)$. However, as far as we know, such an expression does not exist in the literature.

To derive the desired relation, let us consider the asymptotics defined by

$$z \to -\infty, \quad r_\perp = O(|z|^{1/2}), \quad k_\perp = O(|z|^0). \tag{28}$$

In this limit, we have

$$\xi = \frac{r_\perp^2}{2|z|} + O(|z|^{-1}), \quad \eta = 2|z| + \frac{r_\perp^2}{2|z|} + O(|z|^{-1}), \tag{29}$$

and

$$\frac{\psi(\xi,\eta)}{g(z,k_\perp)}\bigg|_{z\to-\infty} = \frac{1}{|z|^{1/2}}\exp\left[\frac{ik_\perp^2|z|^{1/2}}{(2F)^{1/2}} + \frac{iF^{1/2}r_\perp^2}{2|2z|^{1/2}}\right]\phi\left(\frac{r_\perp^2}{2|z|}\right). \tag{30}$$

In addition, the Bessel function in Eq. (27) can be substituted by its asymptotics for large values of the argument. The product of the exponential factor in Eq. (30) and $J_m(k_\perp r_\perp)$ is a rapidly oscillating function with a phase of order $O(|z|^{1/2})$, so the integral in Eq. (27) can be calculated using the steepest descent method. The only saddle point contributing to the integral is located at

$$r_\perp = \frac{k_\perp|2z|^{1/2}}{F^{1/2}}, \tag{31}$$

which agrees with Eq. (28). This point has a simple physical meaning: the coordinate of an ionized electron accelerated by the electric field at large times is $(\mathbf{r}_\perp, z) = (\mathbf{k}_\perp t, -Ft^2/2)$, independently of the initial conditions, which after eliminating the time t leads to Eq. (31). The last factor in Eq. (30) has a phase of order $O(|z|^0)$, so it does not affect the position of the saddle point. Calculating the integral in Eq. (27), we find

$$A(k_\perp) = \frac{2^{3/2}\pi i}{F^{1/2}}\phi\left(\frac{k_\perp^2}{F}\right). \tag{32}$$

The TMD of the ionized electrons is thus given by

$$P(k_\perp) \equiv |A(k_\perp)|^2 = \frac{8\pi^2}{F}\left|\phi\left(\frac{k_\perp^2}{F}\right)\right|^2. \tag{33}$$

This formula is the main analytical result of this work. Taking into account Eq. (20), it expands the TMD in terms of the asymptotic basis $\phi_\nu(\xi)$ and coefficients f_ν. This expansion plays a fundamental role in the present problem as, for example, the partial-wave expansion of a scattering amplitude in scattering theory [21,66]. For the hydrogen atom, only one term is present in the expansion. This is yet another interesting manifestation of the enhanced $O(4)$ symmetry of the Coulomb potential [21,67].

B. Weak-field limit

For a better understanding of the physical meaning of the asymptotic basis $\phi_\nu(\xi)$ and coefficients f_ν introduced in the present formulation, as well as for relating our results to previous studies, it is instructive to consider the deep tunneling regime defined by

$$F \ll \varkappa^3, \quad \varkappa = (2|E_0|)^{1/2}. \tag{34}$$

This regime is characterized by the presence of a wide potential barrier for the motion in η that extends from the atomic core to the outermost turning point $\eta_t \approx -2E_0/F \gg \eta_c$ for Eq. (17). The ionization occurs by tunneling through the barrier. The tunneling probability is exponentially small for $F \to 0$, so we have

$$\Gamma \ll \mathcal{E}. \tag{35}$$

Thus in the presence of a weak electric field the bound atomic state turns into a narrow resonance. It should be noted that resonance is an asymptotic notion which acquires physical meaning only if the condition (35) is satisfied. The SS's representing resonances posses some additional properties which do not hold in the general case [3,4,6]. The eigenfunction $\psi(\mathbf{r})$ in this case is almost real and coincides with the unperturbed bound state in the region $\eta \lesssim \eta_m$, where η_m is defined by $\eta_t \ll \eta_m \ll F/\Gamma^2$. Indeed, as can be seen from Eqs. (18) and (19), which hold for $\eta \gg \eta_t$ and hence are valid for $\eta \sim \eta_m$, the exponential growth of $\psi(\mathbf{r})$ reveals itself only beyond $\eta \sim F/\Gamma^2$. Taking into account Eq. (8), we obtain

$$\int_{\eta\leqslant\eta_m} |\psi(\mathbf{r})|^2 d\mathbf{r} = 1 + O(\Gamma). \tag{36}$$

Integrating both sides of Eq. (22) over the region $\eta \leqslant \eta_m$, substituting into the left-hand side Eqs. (4) and (19), and using Eq. (36), we find

$$\Gamma = \sum_\nu \Gamma_\nu + O(\Gamma^2), \quad \Gamma_\nu = |f_\nu|^2. \tag{37}$$

Thus coefficients f_ν define the partial widths Γ_ν of the SS for ionization into channel ν. Relations similar to Eqs. (36) and (37) hold also for SS's representing resonances in three-body Coulomb systems [13]. On the other hand, integrating both sides of Eq. (22) over the region $z \geqslant -\eta_m/2$ and substituting into the left-hand side Eq. (23), we obtain

$$\int_0^\infty P(k_\perp)\frac{k_\perp dk_\perp}{(2\pi)^2} = \Gamma + O(\Gamma^2). \tag{38}$$

Thus the total outgoing flux is equal to Γ, as one would expect. It can be seen that (37) and (38) agree with the general formula (33), as it should be. We recall that Eqs. (36) through (38) hold only in the limit $F \to 0$, when the condition (35) is satisfied.

For $F = 0$, the solutions to Eq. (16) are given by

$$\beta_\nu|_{F=0} \equiv \beta_\nu^{(0)} = Z_{\mathrm{as}} - \varkappa\left(\nu + \frac{1+|m|}{2}\right), \tag{39a}$$

$$\phi_\nu(\xi)|_{F=0} \equiv \phi_\nu^{(0)}(\xi) = \varkappa^{1/2}s^{|m|/2}e^{-s/2}\tilde{L}_\nu^{(|m|)}(s), \quad s = \varkappa\xi, \tag{39b}$$

where $\tilde{L}_n^{(\alpha)}(x)$ are the normalized generalized Laguerre polynomials [65]. From the semiclassical solution to Eq. (17) in the underbarrier region $\eta_c < \eta < \eta_t$, we obtain

$$f_\nu|_{F\to 0} = \tilde{f}_\nu F^{-\beta_\nu^{(0)}/\varkappa}\exp\left(-\frac{\varkappa^3}{3F}\right), \tag{40}$$

where the coefficients $\tilde{f}_\nu$ do not depend on F. Since $\beta_0^{(0)} > \beta_1^{(0)} > \beta_2^{(0)} \ldots$, the dominant contribution to Eq. (33) for $F \to 0$ comes from the channel with $\nu = 0$, unless it is accidentally $\tilde{f}_0 = 0$. Thus for a general potential of the type (3) in the weak-field limit, the TMD $P(k_\perp)$ as a function of $k_\perp$ takes the form

$$P(k_\perp)|_{F\to 0} \propto k_\perp^{2|m|}\exp\left(-\frac{\varkappa k_\perp^2}{F}\right), \tag{41}$$

and Γ as a function of F behaves as

$$\Gamma|_{F\to 0} \propto F^{1+|m|-2Z_{\mathrm{as}}/\varkappa}\exp\left(-\frac{2\varkappa^3}{3F}\right). \tag{42}$$

From Eqs. (37) and (40), one can also find the partial widths Γ_ν. For the hydrogen atom, the unperturbed bound state is identified by parabolic quantum numbers (n_ξ,n_η,m) [21]. In this case, only one coefficient $\tilde{f}_\nu$ with $\nu = n_\xi$ differs from zero, $\varkappa = 1/n$, where $n = n_\xi + n_\eta + |m| + 1$, and instead of Eqs. (41) and (42) we have

$$P(k_\perp)|_{F\to 0} \propto \left[\phi_{n_\xi}^{(0)}\left(\frac{k_\perp^2}{F}\right)\right]^2, \tag{43}$$

and

$$\Gamma|_{F\to 0} \propto F^{-1-|m|-2n_\eta}\exp\left(-\frac{2}{3n^3F}\right). \tag{44}$$

Equations (43) and (44) coincide with Eqs. (41) and (42), respectively, only for states with $n_\xi = 0$; otherwise, the weak-field behavior of $P(k_\perp)$ and Γ for the hydrogen atom differs from that for other atoms. We do not give explicit expressions for the coefficients in Eqs. (41) through (44), because these equations play only a secondary role in the present work; our primary interest is in the exact results beyond the weak-field limit to be reported in the following.

Equations (41) through (44) can be compared with the results of previous studies. As was mentioned in the Introduction, the asymptotics of Γ for $F \to 0$ was considered by many authors. The basic problem of the hydrogen atom in the ground state was first treated in [22], where the exponential factor in Eq. (44) was obtained. The correct pre-exponential factor $4F^{-1}$ was first obtained using the semiclassical approximation in [21]. The asymptotics of Γ for an arbitrary bound state of the hydrogen atom was obtained in [24]. Equation (44) agrees with the results of [21,24]. Tunneling ionization from a finite-range potential ($Z_{\rm as} = 0$) was first considered in [36]. It was shown that the exponential factor in this case is similar to that for the Coulomb potential, but the pre-exponential factor for the $1s$ state is proportional to F instead of F^{-1}. Equation (42) with $m = 0$ agrees with the results of [36]. We are not aware of any discussions of the TMD in the stationary framework; the available results for $P(k_\perp)$ were obtained in the low-frequency limit of the nonstationary Keldysh theory [41] in [42,43]. Equation (41) with $m = 0$ agrees with the Gaussian shape of the TMD following from the results of [42,43] in the limit $\gamma \to 0$, for details see [44]. This result was reproduced by subsequent authors [46]. In more recent studies, the origin of the theoretical construction [41–43] that has led to Eq. (41) and, more importantly, its limitations were forgotten, and the Gaussian shape of the TMD for ionization by intense laser field was attributed a universal character [68]. The present analysis shows that Eq. (41) is indeed universal, that is, it applies to all atoms, *except* for the hydrogen atom in excited states with $n_\xi \neq 0$ and *only* in the deep tunneling regime (34). We will see in the following that, beyond these limitations, the exact TMD defined by Eq. (33) may qualitatively differ from Eq. (41).

V. ILLUSTRATIVE RESULTS

In practical calculations, instead of solving Eq. (12) obtained by substituting the adiabatic expansion (11) into Eq. (5), it is incomparably more efficient (less time consuming, more accurate, and easier in implementation) to solve Eq. (5) using the slow-variable discretization (SVD) method [55]. The computational procedure used in the present calculations is outlined in the Appendix. In the following we report some illustrative numerical results.

A. Coulomb potential: H

Let us start with a purely Coulomb potential defined by Eq. (3b) with $Z_{\rm as} = 1$ and $\eta_c = 0$, which corresponds to the hydrogen atom. We consider four lowest SS's of H originating from the bound states with $n = 1$ and $n = 2$. The states are labeled by their parabolic quantum numbers (n_ξ,n_η,m) in the limit $F \to 0$. The energies and widths for these states as functions of F are shown in Fig. 1. The energy of the ground state (0,0,0) first goes down, but then begins to rise, having a minimum at $F \approx 0.736$. Among the three states with $n = 2$, the state (0,1,0) extends toward the direction of ionization $z \to -\infty$, so it has the lowest energy and largest width. The opposite is true for the state (1,0,0). The rotationally excited state (0,0,1) behaves intermediately. For all the states, the width monotonically grows with F. There is an extensive literature on calculations of the complex energy eigenvalues for the hydrogen atom in a static electric field [25–34]. For the Coulomb potential, the SVD expansion (A6) contains only one channel, so it is easy to achieve relatively high accuracy of the results. The results shown in Fig. 1 are converged to at least ten significant digits; within this accuracy, they coincide with the results reported in [25–34]. For comparison, we also show the results of the second-order perturbation theory [21] and semiclassical asymptotics [21,24]. One can see that these approximations, which formally apply under the condition (34), are valid quantitatively only at very small F. For example, for the ground state, their error reaches 10% already at $F = 0.26$ and $F = 0.01$ for $\mathcal{E}$ and Γ, respectively. For states with $n = 2$, this happens at about eight times smaller values of F, in accordance with Eq. (34).

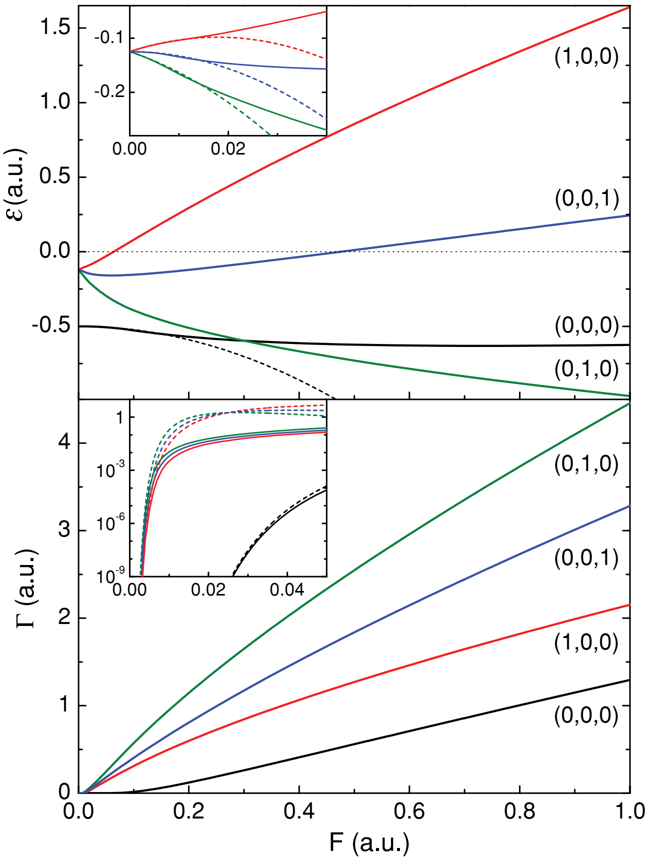

FIG. 1. (Color online) The energy $\mathcal{E}$ and width Γ for four lowest Siegert states of H labeled by parabolic quantum numbers (n_ξ,n_η,m). Solid lines: exact results. Dashed lines: the second-order perturbation theory [21], for $\mathcal{E}$, and semiclassical asymptotics [21,24], for Γ.

For the Coulomb potential, there is only one term in Eq. (20), hence the TMD (33) is defined by the coefficient f_ν and function $\phi_\nu(\xi)$ for a single asymptotic channel. The TMD's for the same four states of H are shown in Fig. 2. To bring the vastly different in magnitude results for the different values of F to a common scale, we divide $P(k_\perp)$ by

$$\mathcal{N} = F^{-1} \int_0^\infty P(k_\perp) k_\perp dk_\perp, \qquad (45)$$

and show it as a function of the scaled argument $k_\perp/F^{1/2}$. Another goal of such a normalization and scaling is to reveal the dependence of the *shape* of the TMD on F, which is defined by the channel function $\phi_\nu(\xi)$, disregarding its *magnitude*

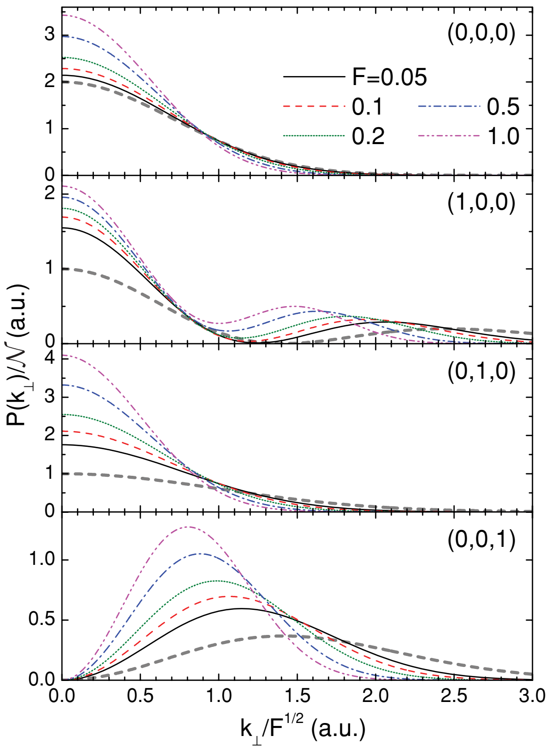

FIG. 2. (Color online) The transverse momentum distributions for the same four states of H as shown in Fig. 1. The normalization factor $\mathcal{N}$ is defined by Eq. (45). Thick dashed lines: the weak-field limit results from Eq. (43).

determined by the coefficient f_ν. If $\phi_\nu(\xi)$ were independent of F, as is the case in the weak-field limit, the different curves for the same state in Fig. 2 would coincide. Indeed, one can see that the TMD's for the different states converge to those defined by Eq. (43) as $F \to 0$, and for the ground state this convergence is faster than for states with $n = 2$. In the weak-field limit, the width of the TMD in $k_\perp$ grows $\propto F^{1/2}$, see Eq. (43). However, for larger values of F, this growth slows down, as can be seen from the fact that the curves in Fig. 2 shrink to the left as F grows. This is explained by the action of the term $F\xi^2/4$ in Eq. (16a), which reduces the extent of the asymptotic channel functions $\phi_\nu(\xi)$ in ξ. In general, Fig. 2 shows that the dependence of the shape of the TMD's on F is rather strong, and only for very weak fields are the results from Eq. (43) correct quantitatively.

B. Potentials with non-Coulombic core: Ne, Ar, Kr, and Xe

Many-electron atoms are often described in the single-active-electron approximation by potentials of the form

$$V(r) = -\frac{Z_{\text{eff}}(r)}{r}, \tag{46}$$

where the effective charge $Z_{\text{eff}}(r)$ monotonically decreases from the bare nuclear charge Z, at $r = 0$, to $Z_{\text{as}} = 1$, at $r \to \infty$. Equation (46) complies with Eq. (3). A simple analytical formula for $Z_{\text{eff}}(r)$ was proposed in [57],

$$Z_{\text{eff}}(r) = Z - (Z-1)\{1 - [(b/a)(e^{ar} - 1) + 1]^{-1}\}. \tag{47}$$

The recommended values of the parameters a and b for the different atoms can be found in [58]. This function exponentially approaches its asymptotic value 1 with the exponent a in the interval 1-2, so Eq. (3b) can be safely imposed in the numerical calculations at $\eta_c \sim 30 - 50$, depending on the accuracy desired.

We consider an electron in the state with $m = 0$ in the outer shells $2p$, $3p$, $4p$, and $5p$ of the noble-gas atoms Ne, Ar, Kr, and Xe, respectively. The binding energies $|E_0|$ in these states obtained using Eqs. (46) and (47) with the parameters from [58] are 0.811, 0.606, 0.459, and 0.486, while the exact ionization potentials are 0.793, 0.579, 0.515, and 0.446, respectively. The error varies from 2% for Ne to 11% for Kr. Such a poor accuracy of the binding energies results from a compromise in attempting to simultaneously reproduce several global atomic properties and is a price for simplicity of this model potential [57,58]. More accurate one-electron potentials are available in the literature [69,70], but for the present illustrative purposes it is sufficient to use the one described above.

The energies and widths for the SS's of the four noble-gas atoms as functions of F are shown in Fig. 3. The energy behaves nonmonotonically. First it goes down, with $|\mathcal{E} - E_0| \propto F^2$, in agreement with the second-order perturbation theory. Then it begins to rise. For Xe, it reaches a maximum at $F \approx 0.37$ and then rapidly goes down again. The same happens for the other atoms at larger values of F; the corresponding

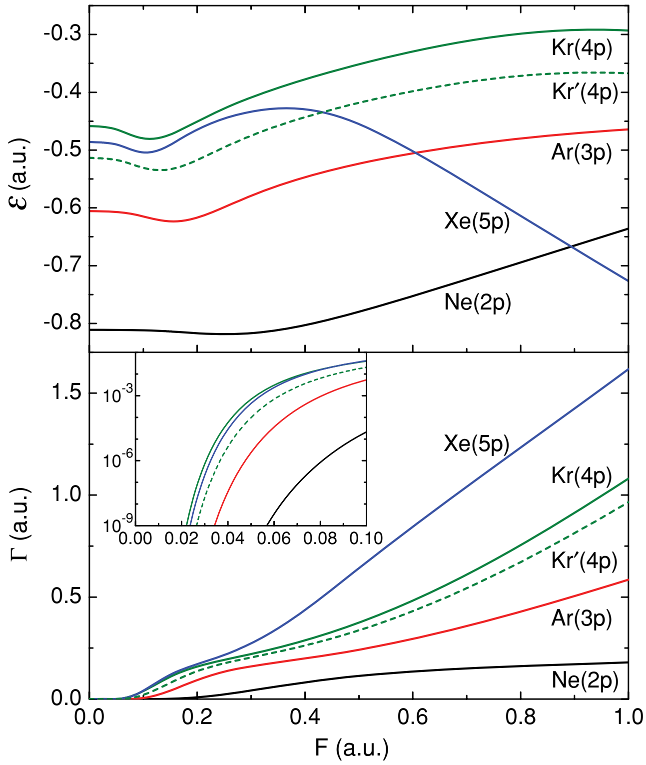

FIG. 3. (Color online) The energy $\mathcal{E}$ and width Γ for the Siegert states of Ne($2p$), Ar($3p$), Kr($4p$), and Xe($5p$) in the single-active-electron approximation with the model potential defined by Eqs. (46) and (47), see Refs. [57,58]. The results labeled by Kr′($4p$) are obtained with slightly modified parameters of the potential.

TABLE I. Convergence of the Siegert eigenvalue $E = \mathcal{E} - i\Gamma/2$ for Ar($3p$) with respect to the number of adiabatic channels N_{ch} in the SVD expansion (A6). All digits in the last line for each value of F are converged. $a(b)$ means $a \times 10^b$.

F	N_{ch}	$-\mathcal{E}$	Γ
0	5	0.600 804	0
	10	0.605 514	0
	15	0.605 671	0
	20	0.605 683	0
	25	0.605 684	0
	30	0.605 685	0
0.05	5	0.603 928	0.270 883(−5)
	10	0.607 101	0.237 055(−5)
	15	0.607 143	0.236 645(−5)
	20	0.607 144	0.236 633(−5)
0.1	5	0.612 559	0.560 766(−2)
	10	0.614 940	0.538 148(−2)
	15	0.614 960	0.537 965(−2)
	20	0.614 961	0.537 961(−2)
0.2	5	0.614 810	0.939 032(−1)
	10	0.616 802	0.931 251(−1)
	15	0.616 812	0.931 216(−1)
	20	0.616 812	0.931 215(−1)
0.5	5	0.522 728	0.242 062
	10	0.523 586	0.241 715
	15	0.523 588	0.241 714
1.0	5	0.463 957	0.585 915
	10	0.464 171	0.585 483
	15	0.464 172	0.585 482

maximum for Kr is located at $F \approx 0.94$. For small F, the width rapidly decreases with the increase of the binding energy $|E_0|$, so the smallest width corresponds to Ne, in agreement with Eq. (42). However, the order of the curves may change for larger F, as is the case for Kr and Xe. In fact, with the parameters from [58], the binding energy of Kr is smaller than that of Xe, which is wrong. By slightly modifying the parameters in Eq. (47) for Kr (1.320 and 4.355 instead of 1.351 and 4.418 for a and b, respectively), we obtain $|E_0| \approx 0.514$, which is much closer to the exact value 0.515 and restores the correct order of the binding energies. The dashed lines in Fig. 3 labeled by Kr$'(4p)$ are obtained with the modified parameters. This illustrates the sensitivity of the results to a variation of the potential.

For non-Coulombic potentials, several adiabatic channels are to be included in the SVD expansion (A6) to obtain converged results. The results shown in Fig. 3 are converged to about six significant digits. The rate of convergence of the Siegert eigenvalue E with respect to the number of channels is illustrated in Table I. The convergence becomes faster for larger F because the relative role of the term with the electric field in Eq. (1) grows, and this term is exactly separable in parabolic coordinates. To put it differently, the extent of the adiabatic basis functions $\phi_\nu(\xi;\eta)$ in ξ decreases as F grows, hence the intervals between the eigenvalues $\beta_\nu(\eta)$ grow, and the nonadiabatic couplings (13) become weaker.

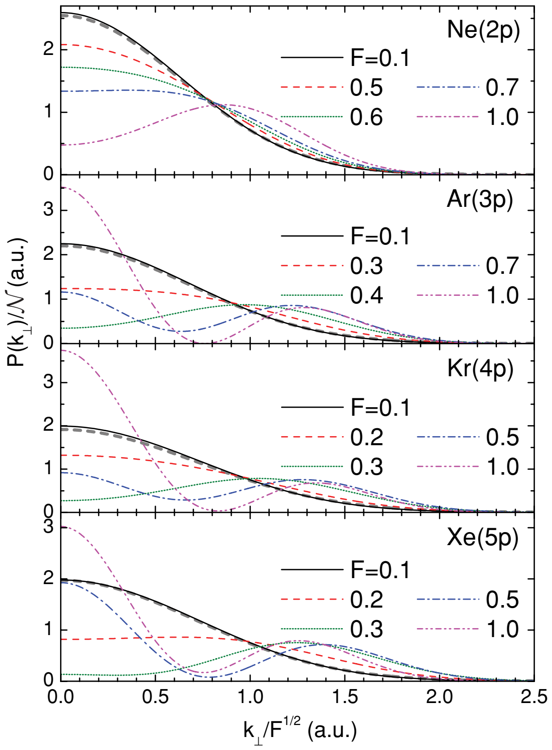

FIG. 4. (Color online) The transverse momentum distributions for the same four atoms as shown in Fig. 3. The normalization factor $\mathcal{N}$ is defined by Eq. (45). Thick dashed lines: the weak-field limit results from Eq. (41).

The TMD's for the noble-gas atoms are shown in Fig. 4. For small F, the results are close to the Gaussian distribution defined by Eq. (41). This corresponds to the situation where the lowest asymptotic channel with $\nu = 0$ gives a dominant contribution to Eqs. (20) and (33). However, for larger F, the behavior of $P(k_\perp)$ becomes nonmonotonic. This is explained by the emergence of a nonnegligible contribution from the channel with $\nu = 1$. The dependence of the coefficients f_ν in Eq. (20) on F is illustrated in Fig. 5. In agreement with the analysis of Sec. IV B, only f_0 survives for $F \to 0$. For larger F, f_1 becomes comparable with f_0. As is seen from Fig. 5, for Ar in the interval of F under consideration, the ionization dominantly occurs in the lowest two channels with $\nu = 0$ and $\nu = 1$; the contributions from higher channels rapidly decay with ν and remain negligible. An interference of the

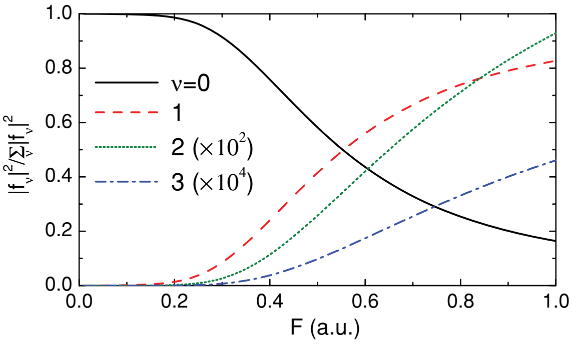

FIG. 5. (Color online) The asymptotic coefficients f_ν for Ar($3p$).

contributions from these two channels results in the behavior seen in Fig. 4. As F grows, the Gaussian shape of $P(k_\perp)$ changes qualitatively: a maximum at $k_\perp = 0$ first turns into a minimum, and then again becomes a maximum. For example, for Ar, a change from a maximum to minimum occurs for the first time between $F = 0.3$ and $F = 0.4$; indeed, this is where f_1 reaches an appreciable value, see Fig. 5. We again conclude that the dependence of the shape of the TMD's on F is rather strong, and for sufficiently large F Eq. (41) becomes wrong qualitatively.

C. Finite-range potential: H$^-$

We finally consider a finite-range potential modeling the force that binds the outer electron in a hydrogen negative ion,

$$V(r) = -V_0 \exp\left(-r^2/r_0^2\right). \tag{48}$$

With the parameters $V_0 = 0.383\,1087$ and $r_0 = 2.5026$, this potential reproduces the correct values of the binding energy $|E_0| = 0.027\,7510$ and s-wave scattering length for the e–H interaction [19]. It was used in [19,20] for the analysis of photodetachment of H$^-$ by high-frequency laser pulses. Equation (48) complies with Eq. (3) with $Z_{\rm as} = 0$ and $\eta_c \sim 20$.

The energy and width for the SS of H$^-$ as functions of F are shown in Fig. 6. The binding energy in the present case is very small, so the effective strength of the electric field $F/\varkappa^3$ for the same value of F is larger than that for neutral atoms, see Eq. (34). The interval where $\mathcal{E}$ depends on F quadratically (the second-order Stark shift) is so narrow that it cannot be seen in the scale of Fig. 6. The width Γ rapidly grows with F and becomes equal to $|\mathcal{E}|$ already at $F = 0.025$. The TMD's for several values of F are shown in Fig. 7. Only for as weak fields as $F = 0.001$ the exact TMD approaches that defined by Eq. (41). For larger F, in contrast to the noble-gas atoms, the TMD for H$^-$ preserves a bell-like shape, but its width is essentially smaller than that following from Eq. (41). Such a difference in the behavior of the shape of the TMD is explained by the relative phase of the first two terms in Eq. (20) near $\xi = 0$, which results in destructive interference, for potentials with a Coulomb tail, and constructive interference, for finite-range potentials.

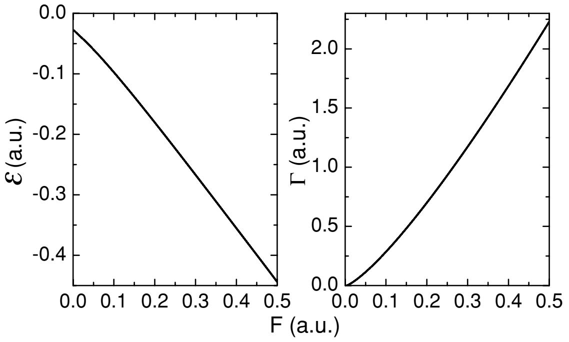

FIG. 6. The energy $\mathcal{E}$ and width Γ for the Siegert state of H$^-$ in the single-active-electron approximation with the model potential defined by Eq. (48).

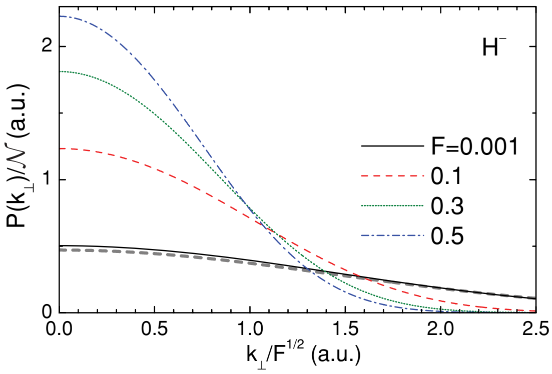

FIG. 7. (Color online) The transverse momentum distributions for H$^-$. The normalization factor $\mathcal{N}$ is defined by Eq. (45). Thick dashed line: the weak-field limit results from Eq. (41).

VI. TRANSVERSE MOMENTUM DISTRIBUTION OF PHOTOELECTRONS IN THE ADIABATIC REGIME

The present study of the atomic SS's in a static electric field is motivated by their applications in the adiabatic theory of ionization of atoms by intense laser pulses [53]. Even though a thorough development of this theory for the three-dimensional case is not finished yet [54], the present work would be incomplete without at least a preliminary illustration of the role played by the SS's in the laser-atom interaction problem. To provide such an illustration, we consider ionization of Ar described by the same one-electron potential as previously by a linearly polarized half-cycle pulse of a time-dependent electric field $\mathbf{F}(t) = F(t)\mathbf{e}_z$, where

$$F(t) = -F_0 \sin^2(\pi t/T), \quad 0 \leqslant t \leqslant T. \tag{49}$$

The pulse amplitude $F_0 = 0.414$ ($I = 6.0 \times 10^{15}$ W/cm^2) is chosen to be well above the boundary $F \approx 0.2$ between the tunneling and overbarrier regimes of ionization for the $3p$ ($m = 0$) state of Ar. We report calculations for the pulse duration $T = 45.48$ (1.1 fs). A characteristic time scale for this pulse can be estimated by $T/2$, so the adiabatic parameter [53] in this case is $\epsilon = 4\pi/(|E_0|T) \approx 0.46$, which is just the onset of the adiabatic regime. We are fully aware that Eq. (49) is far from realistic laser pulses. However, our goal here is to analyze the structure of a single photoelectron wave packet created by a unidirectional pulse of electric field, and to this end Eq. (49) is a quite suitable model.

We solved the time-dependent Schrödinger equation and calculated the two-dimensional photoelectron momentum distribution $P(k_\perp, k_z)$ using a program described in [71,72]; the same program was used in [50–52]. The results are shown in Fig. 8(a). Let us first discuss the extent of this distribution in the longitudinal component k_z of the photoelectron momentum. In the adiabatic regime for the present pulse, there is a one-to-one correspondence between k_z and the moment of ionization t given by the classical equation [53]

$$k_z(t) = -\int_t^T F(t')\,dt', \quad 0 \leqslant t \leqslant T. \tag{50}$$

This equation implies that the photoelectron appears in the continuum at the moment t with zero initial velocity and

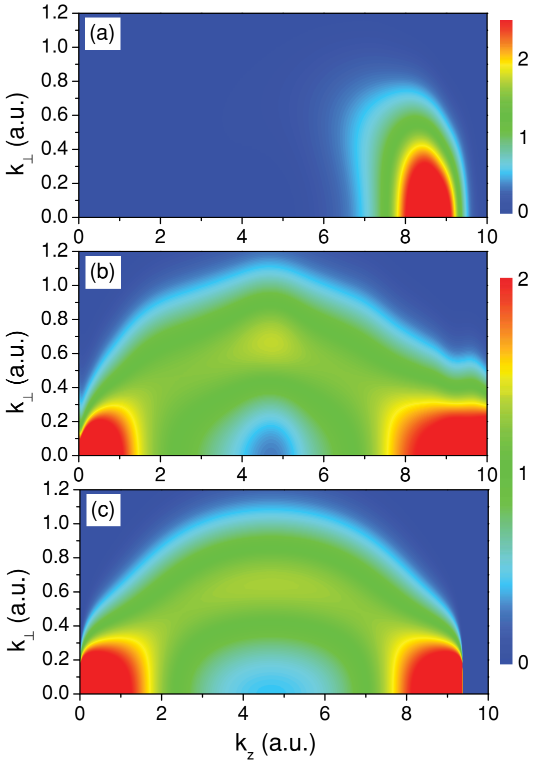

FIG. 8. (Color online) (a) The photoelectron momentum distribution $P(k_\perp,k_z)$ for Ar($3p$) generated by a half-cycle pulse (49) with $F_0 = 0.414$ and $T = 45.48$ obtained by solving the time-dependent Schrödinger equation. (b) The corresponding normalized photoelectron momentum distribution $\tilde{P}(k_\perp,k_z)$ defined by Eq. (51). (c) The normalized photoelectron momentum distribution in the adiabatic approximation obtained from Eqs. (51) and (53).

its further motion is driven only by the electric field. We emphasize that Eq. (50) is not taken for granted, but follows from the adiabatic theory [53]. According to Eq. (50), electrons ionized at earlier (later) stages of the pulse have larger (smaller) values of k_z. Thus the photoelectron momentum distribution must be localized between $k_z(T) = 0$ and $k_z(0) = F_0T/2 \approx 9.41$. Indeed, one can see that $P(k_\perp,k_z)$ rapidly vanishes beyond the upper boundary of this interval. However, this function also decays to the left of a sharp maximum at $(k_\perp,k_z) \approx (0,8.5)$. The latter behavior is explained by depletion. The survival probability for the present pulse is $P_0 = 1.39 \times 10^{-2}$. Almost complete ionization occurs in the initial rising part of the pulse, so the probability to survive until later moments, which contribute to smaller values of k_z in the spectrum, is small.

Equations (49) and (50) establish a correspondence between the longitudinal momentum k_z and the value of the electric field F at the moment of ionization t; this defines a function $F(k_z)$. For example, $k_z = 8.5$ corresponds to $t \approx 11.64$ and $F \approx 0.21$; this is the beginning of the overbarrier regime in the rising part of the pulse. There is another moment $t \approx 33.84$ and momentum $k_z = 0.91$ corresponding to the same value of F; this is the end of the overbarrier regime in the falling part of the pulse. The maximum field $F = F_0 = 0.414$ corresponds to $t = T/2 = 22.74$ and $k_z = F_0T/4 \approx 4.70$. For $k_z > 8.5$, the distribution in $k_\perp$ (i.e., the TMD of the photoelectrons) looks more or less like a Gaussian. We wish to analyze the TMD of the electrons ionized in the essentially overbarrier regime corresponding to the interval $0.91 < k_z < 8.5$. To eliminate the effect of depletion, we normalize the photoelectron momentum distribution shown in Fig. 8(a) for each value of k_z,

$$\tilde{P}(k_\perp,k_z) = \frac{P(k_\perp,k_z)}{\int_0^\infty P(k_\perp,k_z)\, dk_\perp}. \tag{51}$$

This function is shown in Fig. 8(b). Now one can clearly see what happens with the TMD beyond the tunneling regime. The main feature to be noticed in the figure is a dark spot centered at $(k_\perp,k_z) \approx (0,4.70)$. This spot appears because a maximum of $\tilde{P}(k_\perp,k_z)$ as a function of $k_\perp$ at $k_\perp = 0$ turns into a minimum as k_z moves from the upper classical boundary of the spectrum $k_z \approx 9.41$ to 4.70, which corresponds to the rising part of the pulse. This evolution is repeated in the reverse order as k_z moves further to the lower classical boundary of the spectrum $k_z = 0$ in the falling part of the pulse. At the maximum of the pulse, $F = 0.414$ and $k_z \approx 4.70$, the minimum of $\tilde{P}(k_\perp,k_z)$ at $k_\perp = 0$ is most pronounced. The maximum of $\tilde{P}(k_\perp,k_z)$ for this value of k_z is located at $k_\perp \approx 0.7$, which corresponds to $k_\perp/F^{1/2} \approx 1.1$. All these observations agree with the behavior of the TMD for Ar($3p$) as a function of $k_\perp$ and F shown in Fig. 4.

The adiabatic theory [53,54] enables us to elevate this qualitative consideration to a quantitative level. According to this theory, the survival probability is given by

$$P_0 = \exp\left(-\int_0^T \Gamma|_{F=|F(t)|}dt\right) \approx 1.35 \times 10^{-2}, \tag{52}$$

where Γ is the width of the SS originating from the initial bound state of the atom, which should be taken for the momentary absolute value of the electric field. This result is very close to the exact one 1.39×10^{-2}. The photoelectron momentum distribution in the extreme adiabatic regime $\epsilon \to 0$ takes the form

$$P(k_\perp,k_z) \propto P(k_\perp)|_{F=F(k_z)}. \tag{53}$$

Here $P(k_\perp)$ is the TMD for the SS defined by Eq. (33), which should be taken for the value of F that corresponds to the given value of k_z according to Eqs. (49) and (50). The coefficient in Eq. (53) may depend on k_z, but does not depend on $k_\perp$. This coefficient cancels out upon substituting into Eq. (51), so Eq. (53) is sufficient for calculating the normalized photoelectron momentum distribution in the adiabatic approximation. The result is shown in Fig. 8(c). This distribution is symmetric with respect to the line $k_z \approx 4.70$ because of the symmetry of the pulse (49), and vanishes beyond the upper classical boundary of the spectrum $k_z \approx 9.41$. A more careful analysis involving analytic continuation to complex values of F shows [54] that the adiabatic approximation can be extended to the classically inaccessible region $k_z > 9.41$, which, however, goes beyond the scope of the present paper. Apart from this region, one should admit that Figs. 8(b) and 8(c) look very similar. Some visible differences between the exact and adiabatic results can be attributed to the lack of adiabaticity for the present pulse. Thus the TMD of photoelectrons in the adiabatic regime is determined by the TMD for the corresponding SS.

We can now return to a question raised in the Introduction: Do the SS's have some physical meaning in the overbarrier regime? In spite of the artificial character of the pulse defined by Eq. (49) from the standpoint of laser physics, such a pulse is in principle possible, so the photoelectron momentum distribution shown in Fig. 8 is observable. Moreover, when an atom is irradiated by a realistic few-cycle laser pulse of sufficiently high intensity, almost complete ionization occurs during the first unidirectional half-cycle of the field, so the photoelectron wave packet created should be similar to the one shown in Fig. 8. As follows from the present results and will be shown in more detail in [54], the structure of such a wave packet is determined by the properties of the SS. We thus conclude that the atomic SS's in a strong electric field acquire physical meaning in the nonstationary context of the adiabatic theory [53], and their properties are observable experimentally. Of course, this conclusion is restricted by the validity of the single-active-electron approximation.

VII. CONCLUSION

In this paper, we have introduced an efficient method to calculate the atomic Siegert states in a static electric field. The method enables one to obtain the eigenvalue and properly normalized eigenfunction for a selected Siegert state as functions of the electric field for a general class of one-electron atomic potentials. The complex Siegert eigenvalue defines the energy and ionization width of the state, see Eq. (7). An exact expression for the transverse momentum distribution of the ionized electrons in terms of the Siegert eigenfunction in the asymptotic region is derived, see Eqs. (19) and (33). Thus the method yields also the transverse momentum distribution—an important characteristic of the Siegert states that, to the best of our knowledge, was not discussed previously. The method is illustrated by calculations for a number of typical atomic potentials. Although we have considered only spherically symmetric potentials, the method is formulated for a more general class of axially symmetric potentials, so it is capable of treating, e.g., linear molecules aligned along the electric field. By coupling the different m components in the present formulation, the method can be extended to any arbitrarily oriented molecules. This is important for applications development that is in progress.

The ionization of atoms by a static electric field is undoubtedly one of the fundamental problems of atomic physics. The main contribution of the present work to this problem is the analysis of the transverse momentum distribution and Eq. (33). A practical virtue of the atomic Siegert states in an electric field stems from their applications in the adiabatic theory of ionization of atoms by intense laser pulses [53]. The computational method introduced in this work makes the extension of this theory to the three-dimensional case [54] possible.

ACKNOWLEDGMENTS

We thank the participants in the seminars headed by S. Watanabe in Tokyo and M. V. Fedorov in Moscow for useful discussions. O. I. T. thanks the Russian Science Support Foundation for a financial support. This work was supported in part by the PRESTO program of JST, Japan, and by a Grant-in-Aid for Scientific Research (C) from the MEXT, Japan.

APPENDIX: NUMERICAL PROCEDURE

The numerical procedure implementing the approach discussed in the main text and used in the calculations is based on the SVD method [55] in combination with the R-matrix propagation technique [56]. An essential element of this procedure is the discrete variable representation (DVR) [73–75]; all necessary details on constructing DVR's associated with the different types of classical orthogonal polynomials can be found in [76]. A similar procedure is widely used in scattering calculations; see, e.g., [76–83]. However, there are two important differences: (a) the solution of interest here satisfies the outgoing-wave boundary conditions, and (b) here we deal with an eigenvalue problem. These differences deserve a consideration. In the following we briefly discuss the present procedure.

The adiabatic basis. Equations (9) and (16) are solved by expansion in terms of the DVR basis constructed from the generalized Laguerre polynomials $L_n^{(|m|)}(s\xi)$ [76]. This basis exactly incorporates the boundary conditions (9b) and (16b). The scaling factor s defines the extent of the DVR basis functions in ξ; a proper choice of this parameter may accelerate convergence of the expansion. For all states of H and the ground state in non-Coulombic potentials (e.g., for H$^-$) good performance is achieved with $s = \varkappa$, see Eq. (34). For excited states in non-Coulombic potentials [e.g., for Ar($3p$)] because of the coupling with lower adiabatic channels, it is more efficient to use s defined by Eq. (34) with E_0 substituted by something intermediate between E_0 and the energy of the ground state. Further acceleration of the convergence can be achieved by making the choice of s dependent on F.

The inner region, $0 \leqslant \eta \leqslant \eta_c$. The bulk of the calculations is associated with solving Eq. (5) in the inner region. We divide it into N_{sec} sectors with the boundaries at $\bar{\eta}_k$,

$$0 = \bar{\eta}_0 < \bar{\eta}_1 < \cdots < \bar{\eta}_{N_{\text{sec}}} = \eta_c. \tag{A1}$$

Consider the kth sector,

$$\bar{\eta}_- \equiv \bar{\eta}_{k-1} \leqslant \eta \leqslant \bar{\eta}_k \equiv \bar{\eta}_+. \tag{A2}$$

Introduce the Bloch operator [84],

$$\mathcal{L} = \eta\,[\delta(\eta - \bar{\eta}_+) - \delta(\eta - \bar{\eta}_-)]\,\frac{\partial}{\partial\eta}. \tag{A3}$$

The R-matrix basis in the sector is defined by

$$\left[\frac{\partial}{\partial\eta}\eta\frac{\partial}{\partial\eta} - \mathcal{L} - \frac{m^2}{4\eta} + \mathcal{B}(\eta) + \frac{\bar{E}\eta}{2} + \frac{F\eta^2}{4}\right]\bar{\psi}(\xi,\eta) = 0. \tag{A4}$$

This equation differs from Eq. (5) by the term with $\mathcal{L}$, which incorporates the R-matrix boundary conditions. Introduce a new variable x in the sector,

$$\eta(x) = s(x_c + x), \quad -1 \leqslant x \leqslant 1, \tag{A5a}$$

$$s = \frac{\bar{\eta}_+ - \bar{\eta}_-}{2}, \quad x_c = \frac{\bar{\eta}_+ + \bar{\eta}_-}{\bar{\eta}_+ - \bar{\eta}_-}. \tag{A5b}$$

Let x_i and $\pi_i(x)$, $i = 1, \ldots, N_{\rm DVR}$, be the Gaussian quadrature points and DVR basis functions compatible with the boundary conditions for the solution to Eq. (5) at the ends of the sector, and $\eta_i = \eta(x_i)$. In the first sector, to incorporate the regularity boundary conditions (14), the DVR basis is constructed from the Jacobi polynomials $P_n^{(0,|m|)}(x)$; in all subsequent sectors, we use the Legendre polynomials $P_n(x)$ [76]. The solutions to Eq. (A4) are sought in the form of the SVD expansion [55]

$$\bar{\psi}(\xi,\eta) = \sum_{i=1}^{N_{\rm DVR}} \sum_{\nu=1}^{N_{\rm ch}} c_{i\nu} \pi_i(x) \phi_\nu(\xi;\eta_i), \tag{A6}$$

where $N_{\rm ch}$ is the number of adiabatic channels included in the calculations. Substituting this expansion into Eq. (A4), one obtains an algebraic SVD eigenvalue problem,

$$\sum_{j\mu} K_{ij} O_{i\nu,j\mu} c_{j\mu} - \left[\beta_\nu(\eta_i) + \frac{\bar{E}\eta_i}{2} + \frac{F\eta_i^2}{4}\right] c_{i\nu} = 0, \tag{A7}$$

where K_{ij} is the DVR kinetic energy matrix,

$$\begin{aligned} K_{ij} = \frac{1}{s^2} \int_{-1}^{1} \frac{d\pi_i(x)}{dx} \eta(x) \frac{d\pi_j(x)}{dx}\, dx \\ + \int_{-1}^{1} \pi_i(x) \frac{m^2}{4\eta(x)} \pi_j(x)\, dx, \end{aligned} \tag{A8}$$

and $O_{i\nu,j\mu}$ is the overlap matrix for the adiabatic bases at the different quadrature points,

$$O_{i\nu,j\mu} = \langle \phi_\nu(\xi;\eta_i) | \phi_\mu(\xi;\eta_j) \rangle. \tag{A9}$$

The DVR matrix (A8) can be calculated analytically using the formulas given in [76]; the overlap matrix (A9) is calculated numerically using the Gaussian quadrature defining the Laguerre DVR in ξ. The eigenvalues and eigenvectors of Eq. (A7) and the corresponding solutions to Eq. (A4) will be denoted by

$$\bar{E}_n, \quad c_{i\nu}^n, \quad \bar{\psi}_n(\xi,\eta), \quad n = 1,2,\ldots,N_{\rm SVD}, \tag{A10}$$

where $N_{\rm SVD} = N_{\rm DVR} N_{\rm ch}$. The solutions are orthogonal in the region (2a) and (A2) with the weight η. We normalize them by

$$\int_{\bar{\eta}_-}^{\bar{\eta}_+} \langle \bar{\psi}_n(\xi,\eta) | \bar{\psi}_m(\xi,\eta) \rangle \eta d\eta = s \sum_{i\nu} c_{i\nu}^n c_{i\nu}^m \eta_i = \delta_{nm}. \tag{A11}$$

Let $\mathbf{R}(\eta;E)$ denote the R-matrix [85] for the solutions to Eq. (5) defined with respect to the adiabatic basis; the defining equation reads

$$\langle \phi_\nu(\xi;\eta) | \psi(\xi,\eta) \rangle = \sum_\mu R_{\nu\mu}(\eta;E) \left\langle \phi_\mu(\xi;\eta) \middle| \frac{\partial \psi(\xi,\eta)}{\partial \eta} \right\rangle. \tag{A12}$$

Using the solutions to Eq. (A7), one can propagate $\mathbf{R}(\eta;E)$ through the sector. The propagation is accomplished by means of the equation [56]

$$\mathbf{R}(\bar{\eta}_\pm;E) = \pm\mathcal{R}^{(\pm,\pm)} - \mathcal{R}^{(\pm,\mp)}[\mathbf{R}(\bar{\eta}_\mp;E) \pm \mathcal{R}^{(\mp,\mp)}]^{-1}\mathcal{R}^{(\mp,\pm)}, \tag{A13}$$

where the matrices $\mathcal{R}^{(\pm,\pm)}$ are given by

$$\mathcal{R}_{\nu\mu}^{(\pm,\pm)} = 2 \sum_{n=1}^{N_{\rm SVD}} \frac{\bar{f}_\nu^n(\bar{\eta}_\pm) \bar{f}_\mu^n(\bar{\eta}_\pm)}{\bar{E}_n - E}. \tag{A14}$$

Here

$$\begin{aligned} \bar{f}_\nu^n(\bar{\eta}_\pm) &= \bar{\eta}_\pm^{1/2} \langle \phi_\nu(\xi;\bar{\eta}_\pm) | \bar{\psi}_n(\xi;\bar{\eta}_\pm) \rangle \\ &= \bar{\eta}_\pm^{1/2} \sum_{j\mu} c_{j\mu}^n \pi_j(\pm 1) O_{\nu,j\mu}^\pm, \end{aligned} \tag{A15}$$

are the surface amplitudes of the R-matrix eigenfunctions, and

$$O_{\nu,j\mu}^\pm = \langle \phi_\nu(\xi;\bar{\eta}_\pm) | \phi_\mu(\xi;\eta_j) \rangle, \tag{A16}$$

are the surface overlap matrices. Solving Eq. (A7) for each sector in the inner region (A1) and applying Eq. (A13), one can propagate $\mathbf{R}(\eta;E)$ between any two boundary points $\bar{\eta}_k$. We also have

$$\begin{aligned} &\left. \left\langle \phi_\nu(\xi;\eta) \middle| \frac{\partial \psi(\xi,\eta)}{\partial \eta} \right\rangle \right|_{\eta=\bar{\eta}_\pm} \\ &\quad = \sum_\mu D_{\nu\mu}^{(\pm)}(E) \left. \left\langle \phi_\mu(\xi;\eta) \middle| \frac{\partial \psi(\xi,\eta)}{\partial \eta} \right\rangle \right|_{\eta=\bar{\eta}_\mp}, \end{aligned} \tag{A17}$$

where

$$\mathbf{D}^{(\pm)}(E) = \mp \left(\frac{\bar{\eta}_\mp}{\bar{\eta}_\pm}\right)^{1/2} [\mathbf{R}(\bar{\eta}_\pm;E) \mp \mathcal{R}^{(\pm,\pm)}]^{-1} \mathcal{R}^{(\pm,\mp)}. \tag{A18}$$

The outer region, $\eta > \eta_c$. Here, Eq. (5) reduces to uncoupled equations (17) which can be solved by the standard fourth-order Runge-Kutta method [86]. However, it is difficult to achieve high accuracy in the calculations by applying the outgoing-wave boundary condition (18) on the real axis because the solution rapidly oscillates and approaches this asymptotics very slowly. The way of resolving this difficulty is an important technical novelty of the present procedure. We solve Eq. (17) along the steepest descent contour $\tilde{\mathcal{C}}$ defined by

$${\rm Re} \int_{\eta_c}^{\eta} \left[\frac{1-m^2}{4\eta'^2} + \frac{\beta_\nu}{\eta'} + \frac{E}{2} + \frac{F\eta'}{4}\right]^{1/2} d\eta' = 0 \to \eta \in \tilde{\mathcal{C}}. \tag{A19}$$

This contour begins at $\eta = \eta_c$ and runs to infinity parallel to the ray $\arg \eta = \pi/3$, hence Eqs. (18) amount to zero asymptotic boundary condition for $f_\nu(\eta)$ on $\tilde{\mathcal{C}}$. We start from a point $\eta_\infty \in \tilde{\mathcal{C}}$, for which the integral in Eq. (A19) has a sufficiently large value, and propagate the solution of Eq. (17) along $\tilde{\mathcal{C}}$ to η_c by the Runge-Kutta method. Because of the finite accuracy of the calculations, independently of the initial conditions for $f_\nu(\eta)$, only the exponentially growing solution (i.e., the one we need) survives in the propagation. Remarkably, this well-known numerical instability, which usually causes problems in calculations, plays a positive role in the present case. We thus obtain the solutions to Eqs. (17) and (18) up to yet unknown constant coefficients. At a later stage of the calculations, we use $\tilde{\mathcal{C}}$ instead of the complex part of the contour (21) for normalization of the SS.

The matching condition. From Eq. (14), for the regular solutions to Eq. (5) we have

$$R_{\nu\mu}(0;E) = 0. \tag{A20}$$

From the fact that Eq. (12) become uncoupled in the outer region $\eta > \eta_c$, for the outgoing-wave solutions to Eq. (5) we have

$$R_{\nu\mu}(\eta_c;E) = r_\nu \delta_{\nu\mu}, \quad r_\nu = \left.\frac{f_\nu(\eta)}{f'_\nu(\eta)}\right|_{\eta=\eta_c}, \tag{A21}$$

were r_ν, $\nu = 0,\dots,N_{\mathrm{ch}}$, are defined by the solutions to Eqs. (17) and (18) discussed previously. Equations (A20) and (A21) provide the boundary conditions for the R-matrix propagation. Starting from Eq. (A20) and propagating $\mathbf{R}(\eta;E)$ through k sectors to the right, we obtain $\mathbf{R}_{\mathrm{left}}(\bar{\eta}_k;E)$. On the other hand, starting from Eq. (A21) and propagating $\mathbf{R}(\eta;E)$ through $N_{\mathrm{sec}} - k$ sectors to the left, we obtain $\mathbf{R}_{\mathrm{right}}(\bar{\eta}_k;E)$. The requirement of continuity of the solution to Eq. (5) and its derivative with respect to η at $\eta = \bar{\eta}_k$ leads to the matching condition

$$\det[\mathbf{R}_{\mathrm{left}}(\bar{\eta}_k;E) - \mathbf{R}_{\mathrm{right}}(\bar{\eta}_k;E)] = 0. \tag{A22}$$

The values of E for which this equation is satisfied are the Siegert eigenvalues. We solve Eq. (A22) iteratively, starting from the known solution $E = E_0$ for the selected SS for $F = 0$ and incrementing F by sufficiently small steps. At each step, we seek the zero of the smallest eigenvalue of the matrix in Eq. (A22) closest to the solution E found in the previous step using the Newton method [86]. The eigenfunction $\psi(\xi,\eta)$ is then constructed by propagating the corresponding eigenvector using Eqs. (A12), (A13), (A17), and (A18). Applying the normalization condition (8), we finally obtain the asymptotic coefficients f_ν in Eq. (18a). In this way, the SS can be analytically continued to any value of F. We note that this procedure works also for complex F, which is essential for its applications in the adiabatic theory [53,54].

---

[1] G. Gamow, Z. Phys. **51**, 204 (1928).
[2] A. J. F. Siegert, Phys. Rev. **56**, 750 (1939).
[3] O. I. Tolstikhin, V. N. Ostrovsky, and H. Nakamura, Phys. Rev. A **58**, 2077 (1998).
[4] G. V. Sitnikov and O. I. Tolstikhin, Phys. Rev. A **67**, 032714 (2003).
[5] K. Toyota, T. Morishita, and S. Watanabe, Phys. Rev. A **72**, 062718 (2005).
[6] P. A. Batishchev and O. I. Tolstikhin, Phys. Rev. A **75**, 062704 (2007).
[7] O. I. Tolstikhin, V. N. Ostrovsky, and H. Nakamura, Phys. Rev. Lett. **79**, 2026 (1997).
[8] O. I. Tolstikhin, I. Yu. Tolstikhina, and C. Namba, Phys. Rev. A **60**, 4673 (1999).
[9] E. L. Hamilton and C. H. Greene, Phys. Rev. Lett. **89**, 263003 (2002).
[10] K. Toyota and S. Watanabe, Phys. Rev. A **68**, 062504 (2003).
[11] V. Kokoouline and C. H. Greene, Phys. Rev. Lett. **90**, 133201 (2003); Phys. Rev. A **68**, 012703 (2003); **69**, 032711 (2004).
[12] Å. Larson, S. Tonzani, R. Santra, and C. H Greene, J. Phys. Conf. Ser. **4**, 148 (2005).
[13] G. V. Sitnikov and O. I. Tolstikhin, Phys. Rev. A **71**, 022708 (2005).
[14] V. N. Ostrovsky and N. Elander, Phys. Rev. A **71**, 052707 (2005); Chem. Phys. Lett. **411**, 155 (2005).
[15] R. Čurík and C. H. Greene, Phys. Rev. Lett. **98**, 173201 (2007); Mol. Phys. **105**, 1565 (2007).
[16] A. Das, E. D. Poliakoff, R. R. Lucchese, and J. D. Bozek, J. Chem. Phys. **130**, 044302 (2009).
[17] A. del Campo, G. García-Calderón, and J. G. Muga, Phys. Rep. **476**, 1 (2009).
[18] R. Santra, J. M. Shainline, and C. H. Greene, Phys. Rev. A **71**, 032703 (2005).
[19] O. I. Tolstikhin, Phys. Rev. A **73**, 062705 (2006); **74**, 042719 (2006); **77**, 032711 (2008); **77**, 032712 (2008).
[20] K. Toyota, O. I. Tolstikhin, T. Morishita, and S. Watanabe, Phys. Rev. A **76**, 043418 (2007); **78**, 033432 (2008); Phys. Rev. Lett. **103**, 153003 (2009).
[21] L. D. Landau and E. M. Lifshitz, *Quantum Mechanics (Non-relativistic Theory)* (Pergamon Press, Oxford, 1977).
[22] J. R. Oppenheimer, Phys. Rev. **31**, 66 (1928).
[23] C. Lanczos, Z. Phys. **62**, 518 (1930); **65**, 431 (1930); **68**, 204 (1931).
[24] T. Yamabe, A. Tachibana, and H. J. Silverstone, Phys. Rev. A **16**, 877 (1977).
[25] M. H. Alexander, Phys. Rev. **178**, 34 (1969).
[26] M. Hehenberger, H. V. McIntosh, and E. Brändas, Phys. Rev. A **10**, 1494 (1974).
[27] R. J. Damburg and V. V. Kolosov, J. Phys. B **9**, 3149 (1976); **11**, 1921 (1978).
[28] C. Cerjan, R. Hedges, C. Holt, W. P. Reinhardt, K. Scheibner, and J. J. Wendoloski, Int. J. Quantum Chem. **14**, 393 (1978).
[29] H. J. Silverstone, B. G. Adams, J. Cizek, and P. Otto, Phys. Rev. Lett. **43**, 1498 (1979).
[30] L. Benassi and V. Grecchi, J. Phys. B **13**, 911 (1980).
[31] A. Maquet, S. I. Chu, and W. P. Reinhardt, Phys. Rev. A **27**, 2946 (1983).
[32] V. Franceschini, V. Grecchi, and H. J. Silverstone, Phys. Rev. A **32**, 1338 (1985).
[33] C. A. Nicolaides and S. I. Themelis, Phys. Rev. A **45**, 349 (1992).
[34] U. D. Jentschura, Phys. Rev. A **64**, 013403 (2001).
[35] G. Alvarez and H. J. Silverstone, Phys. Rev. A **50**, 4679 (1994).
[36] Yu. N. Demkov and G. F. Drukarev, Zh. Eksp. Teor. Fiz. **47**, 918 (1964) [Sov. Phys. JETP **20**, 614 (1964)].
[37] N. A. Guschina and V. K. Nikulin, Chem. Phys. **10**, 23 (1975).
[38] Yu. N. Demkov and V. N. Ostrovskii, *Zero-Range Potentials and Their Applications in Atomic Physics* (Plenum Press, New York, 1988).
[39] W. P. Reinhardt, Annu. Rev. Phys. Chem. **33**, 223 (1982).
[40] X. M. Tong and C. D. Lin, J. Phys. B **38**, 259 (2005).
[41] L. V. Keldysh, Zh. Eksp. Teor. Fiz. **47**, 1945 (1964) [Sov. Phys. JETP **20**, 1307 (1965)].
[42] A. I. Nikishov and V. I. Ritus, Zh. Eksp. Teor. Fiz. **50**, 255 (1966) [Sov. Phys. JETP **23**, 162 (1966)].

[43] A. M. Perelomov, V. S. Popov, and M. V. Terent'ev, Zh. Eksp. Teor. Fiz. **50**, 1393 (1966) [Sov. Phys. JETP **23**, 924 (1966)]; Zh. Eksp. Teor. Fiz. **51**, 309 (1966) [Sov. Phys. JETP **24**, 207 (1967)].

[44] V. S. Popov, Usp. Fiz. Nauk **174**, 921 (2004) [Phys. Usp. **47**, 855 (2004)].

[45] M. V. Ammosov, N. B. Delone, and V. P. Krainov, Zh. Eksp. Teor. Fiz. **91**, 2008 (1986) [Sov. Phys. JETP **64**, 1191 (1986)].

[46] N. B. Delone and V. P. Krainov, J. Opt. Soc. Am. B **8**, 1207 (1991).

[47] V. S. Popov, Usp. Fiz. Nauk **169**, 819 (1999) [Phys. Usp. **42**, 733 (1999)].

[48] A. Scrinzi, M. Yu. Ivanov, R. Kienberger, and D. M. Villeneuve, J. Phys. B **39**, R1 (2006).

[49] D. B. Milošević, G. G. Paulus, D. Baur, and W. Becker, J. Phys. B **39**, R203 (2006).

[50] T. Morishita, A.-T. Le, Z. Chen, and C. D. Lin, Phys. Rev. Lett. **100**, 013903 (2008).

[51] T. Morishita, A.-T. Le, Z. Chen, and C. D. Lin, New J. Phys. **10**, 025011 (2008).

[52] T. Morishita, T. Umegaki, S. Watanabe, and C. D. Lin, J. Phys.: Conf. Ser. **194**, 012011 (2009).

[53] O. I. Tolstikhin, T. Morishita, and S. Watanabe, Phys. Rev. A **81**, 033415 (2010).

[54] O. I. Tolstikhin and T. Morishita (unpublished).

[55] O. I. Tolstikhin, S. Watanabe, and M. Matsuzawa, J. Phys. B **29**, L389 (1996).

[56] K. L. Baluja, P. G. Burke, and L. A. Morgan, Comput. Phys. Commun. **27**, 299 (1982).

[57] A. E. S. Green, D. L. Sellin, and A. S. Zachor, Phys. Rev. **184**, 1 (1969).

[58] R. H. Garvey, C. H. Jackman, and A. E. S. Green, Phys. Rev. A **12**, 1144 (1975).

[59] M. Born and R. Oppenheimer, Ann. Phys. (Leipzig) **84**, 457 (1927).

[60] J. Macek, J. Phys. B **1**, 831 (1968).

[61] C. D. Lin, Adv. At. Mol. Phys. **22**, 77 (1986); Phys. Rep. **257**, 1 (1995).

[62] A. Kupperman and P. G. Hipes, J. Chem. Phys. **84**, 5962 (1986).

[63] R. T. Pack and G. A. Parker, J. Chem. Phys. **87**, 3888 (1987).

[64] É. É. Shnol, Teor. Mat. Fiz. **8**, 140 (1971) [Theor. Math. Phys. **8**, 729 (1971)].

[65] *Handbook of Mathematical Functions*, edited by M. Abramowitz and I. A. Stegun (Dover Publications, New York, 1972).

[66] R. G. Newton, *Scattering Theory of Waves and Particles* (Springer-Verlag, New York, 1982).

[67] V. A. Fock, Izv. Akad. Nauk SSSR N **2**, 169 (1935); Z. Physik **98**, 145 (1935).

[68] M. Yu. Ivanov, M. Spanner, and O. Smirnova, J. Mod. Opt. **52**, 165 (2005).

[69] R. G. Parr and Y. Weitao, *Density-Functional Theory of Atoms and Molecules* (Oxford University Press, Oxford, 1989).

[70] *Modern techniques in computational chemistry: MOTECC-91*, edited by E. Clementi, (Escom, Leiden, 1991).

[71] Z. Chen, T. Morishita, A.-T. Le, M. Wickenhauser, X. M. Tong, and C. D. Lin, Phys. Rev. A **74**, 053405 (2006).

[72] T. Morishita, Z. Chen, S. Watanabe, and C. D. Lin, Phys. Rev. A **75**, 023407 (2007).

[73] D. O. Harris, G. G. Engerholm, and W. D. Gwinn, J. Chem. Phys. **43**, 1515 (1965).

[74] A. S. Dickinson and P. R. Certain, J. Chem. Phys. **49**, 4209 (1968).

[75] J. C. Light, I. P. Hamilton, and J. V. Lill, J. Chem. Phys. **82**, 1400 (1985).

[76] O. I. Tolstikhin and C. Namba, *CTBC—A Program to Solve the Collinear Three-Body Coulomb Problem: Bound States and Scattering Below the Three-Body Disintegration Threshold*, Research Report NIFS-779 (National Institute for Fusion Science, Toki, Japan, 2003). Available at [http://www.nifs.ac.jp/report/nifs779.html].

[77] D. Kato and S. Watanabe, Phys. Rev. A **56**, 3687 (1997).

[78] O. I. Tolstikhin and H. Nakamura, J. Chem. Phys. **108**, 8899 (1998).

[79] C.-N. Liu, A.-T. Le, T. Morishita, B. D. Esry, and C. D. Lin, Phys. Rev. A **67**, 052705 (2003).

[80] O. I. Tolstikhin and C. Namba, Phys. Rev. A **70**, 062721 (2004).

[81] A.-T. Le, M. W. J. Bromley, and C. D. Lin, Phys. Rev. A **71**, 032713 (2005).

[82] P. Barragán, A.-T. Le, and C. D. Lin, Phys. Rev. A **74**, 012720 (2006).

[83] J. Xu, A.-T. Le, T. Morishita, and C. D. Lin, Phys. Rev. A **78**, 012701 (2008).

[84] C. Bloch, Nucl. Phys. **4**, 503 (1957).

[85] E. P. Wigner and L. Eisenbud, Phys. Rev. **72**, 29 (1947).

[86] W. H. Press, S. A. Teukolsky, W. T. Vetterling, and B. P. Flannery, *Numerical Recipes in FORTRAN* (Cambridge University Press, Cambridge, England, 1992).